Journal of Alloys and Compounds 505 (2010) 194–200

Contents lists available at ScienceDirect

Journal of Alloys and Compounds

journal homepage: www.elsevier.com/locate/jallcom

Mesoporous gadolinium doped titania photocatalyst through an aqueous sol–gel method

K.V. Baiju[a,b], P. Periyat[c], P. Shajesh[a], W. Wunderlich[d], K.A. Manjumol[a], V.S. Smitha[a], K.B. Jaimy[a], K.G.K. Warrier[a,*]

[a] Materials and Minerals Division, National Institute for Interdisciplinary Science & Technology (NIIST), CSIR, Pappanamcode, Thiruvananthapuram 695019, India
[b] Institute of Catalysis and Energy Processing, Northwestern University, USA
[c] Materials and Surface Science Institute (MSSI), The University of Limerick, Ireland
[d] Tokai University, Fac. Engr., Department of Material Science, Kanagawa 259-1292, Japan

ARTICLE INFO

Article history:
Received 30 October 2009
Received in revised form 1 June 2010
Accepted 10 June 2010
Available online 16 June 2010

Keywords:
Sol–gel
Titanyl oxysulphate
Photocatalyst
Anatase
Mesoporous

ABSTRACT

A surfactant-free, aqueous sol–gel synthetic route to a thermally stable gadolinium doped mesoporous nanocrystalline titania is reported for the first time. The mesoporosity was revealed using BET surface area measurements and the pores are stable at temperatures as high as 800 °C. The 2 mol% gadolinium doped titania calcined at 800 °C, displayed a specific surface area of 22 $m^2 g^{-1}$ and a total pore volume 0.142 $cm^3 g^{-1}$, whereas undoped titania is non-porous and has a surface area value as low as 0.3364 $m^2 g^{-1}$ and total pore volume of 0.00096 $cm^3 g^{-1}$. The thermal stability of the anatase phase up to 800 °C was achieved due to the reduction of crystallite size as a result of gadolinium doping in the titania lattice. Transmission electron micrographs showed that the crystallite size of 2 mol% gadolinium doped titania is 20 nm at 800 °C, whereas undoped titania had a crystallite size of 43 nm at the same temperature. The Bronsted acidity of doped titania was further studied using 2,6-dimethyl pyridine adsorption studies. Finally the photocatalytic performance of this mesoporous TiO_2 was analysed using methylene blue degradation and revealed a significantly higher activity than the undoped titania, a factor attributed to the mesoporosity, higher surface area and thermal stability of anatase phase.

1. Introduction

Titanium dioxide is of great scientific and commercial interest due to its widespread use in various fields such as pigments, electronic materials, and catalytic supports [1]. Recently its applications were diversified into self-cleaning coatings [2] and environmental clean-up by virtue of the degradation of industrial organic contaminants due to titanias photon-induced electron transfer properties [3]. A considerable number of reports detail the increase in the photocatalytic activity of titania by doping with metal and non-metal ions. Non-metal dopants such as nitrogen, sulphur, phosphorus and carbon have recently been shown to increase visible light photocatalytic activity and the anatase stability of titania [4–9]. Previously the influences of various metal ion/metal oxide dopants such as Al^{3+}, SiO_2, Ta^{5+}, Nb^{5+}, Cr^{3+}, Si^{4+}, WO_3, CeO_2, Sb and ZnO were studied and were also found to improve the photocatalytic and anatase phase stability of titania [10–20]. These reports showed that the photocatalytic activity of titania depends on a number of factors including; surface area, porosity, phase assembly (preferably the anatase phase), crystallite size, crystallinity, absorption properties of the dyes on the surface of TiO_2, rate of electron hole recombination and the number of electrons/hole created [16–21].

In synthetic titania, the anatase to rutile transformation usually takes place at 400–600 °C [10–21]. Recent literature reports show that lanthanide ion doping increases the anatase to rutile transformation temperature and photocatalytic activity of titania [22–31]. The ability of lanthanides to form complexes with various Lewis bases *e.g.* acids, amines, aldehydes, alcohols, thiols, *etc.* can be effectively used to increase the efficiency of photocatalytic reactions. Incorporation of gadolinium ions into a titania matrix could provide a means to concentrate the organic pollutant at the semiconductor surface and therefore enhance the photo-activity of titania [22]. Recently Nguyen-Phan et al. observed the higher adsorption capacity of benzene over lanthanide doped titania [32]. Moreover, rare earth doped titania is recieving considerable interest due to its photoluminescent property, in which titania absorbs light and transfers it to the rare earth ions [33–36].

Mesoporous titania thin films have the characteristics of an ideal host matrix as the TiO_2 material absorbs strongly and transfers energy efficiently to the weakly absorbing rare earth ions. They are also stable in environmental conditions such as moisture and temperature [34,35]. The preparation of mesoporous gadolinium

* Corresponding author. Tel.: +91 471 490 674; fax: +91 471 491 712.
E-mail address: wwarrierkgk@yahoo.co.in (K.G.K. Warrier).

0925-8388/$ – see front matter © 2010 Elsevier B.V. All rights reserved.
doi:10.1016/j.jallcom.2010.06.028

doped titania is expected to result in a more photocatalytic material due to the interfacial charge transfer to its 4f shells and the elimination of electron hole recombination. Gd doping is proven to be effective in trapping the excited electron and hence, enhancing the electron–hole separation [37]. Recently Mohamed and Mkhalid observed increased photodegradation of EDTA using 3 at. wt.% of rare earth doped (Nd, Sm, Gd, and La) titania–silica composites [24]. Zhu et al. also reported the use of rare earth dopants (Sm^{3+}, Nd^{3+}, Ce^{3+} and Pr^{3+}) in titania–silica composites for methyne blue degradation studies [38]. The effect of Gd_2O_3 in anatase to rutile phase transformation has been reported by Hishita et al. [39] and Zhao et al. [40]. They used a surfactant mediated synthesis for the preparation of gadolinium doped titania. The anatase phase stability and photocatalytic activity of alkoxide derived Gd^{3+} doped titania was reported [41–43]. However, a detailed study of the textural property, which is an important factor to explain the photocatalytic activity, was not presented. The photocatalytic evolution of hydrogen from water using gadolinium doped titania was studied [44]. Hafez et al. demonstrated the photovoltaic application of titania nanotubes doped with the Gd^{3+} ion [45]. The photocatalytic study on high temperature calcined Gd^{3+} doped titania system was again, not reported in the literature.

In this work, an aqueous sol–gel method to synthesise a high temperature stable (above 800 °C) mesoporous gadolinium doped titania without the use of surfactant is reported. This systematic study using different mol% of Gd^{3+} ion doping in the titania matrix describes the effect of doping on the anatase to rutile phase transformation, along with textural properties and photocatalytic activity of titania.

2. Experimental

Titania sol is prepared from titanyl oxysulphate ($TiOSO_4$, Aldrich, 99.99% purity) as previously reported [13]. Gadolinium nitrate (Aldrich, 99.99% purity) solutions corresponding to 1, 2, 5 and 10 mol% of gadolinium were added dropwise to the titania sol in separate batches and stirred for a period of 1 h. The sols were concentrated over a steam bath and subsequently dried in an electric hot air oven at 70 °C to obtain the xerogel, then calcined at different temperatures (500, 600, 700, 800, 850, 900 and 1000 °C) at a heating rate of 10 °C min^{-1} and remaining at the peak temperature for 1 h.

The surface area measurements and pore size analysis were carried out by nitrogen adsorption using Micromeritics Gemini 2375 surface area analyser after degassing each sample at 200 °C for 2 h. XRD patterns of the calcined gels were taken in a Philips X'pertpro X-ray diffractometer in the diffraction angle 2θ range 20–60° using CuKα radiation. The amount of rutile in the sample was estimated using the Spurr (Eq. (1)) [46].

$$F_R = \left(\frac{1}{1 + 0.8(I_A(1\ 0\ 1)/I_R(1\ 1\ 0)}\right) 100 \quad (1)$$

where F_R is the mass fraction of rutile in the sample and I_A (1 0 1) and I_R (1 1 0) are the integrated main peak intensities of anatase and rutile respectively. The crystallite size was calculated using Scherrer formula (Eq. (2)) [47].

$$\Phi = \frac{K\lambda}{\beta \cos\theta} \quad (2)$$

where Φ is the crystallite size, K is the shape factor, λ is the X-ray radiation wavelength and β is the full line width at half-maximum height of the main intensity peak after subtraction of equipment line broadening.

The TEM images of the calcined titania powder were obtained on a Hitachi HF 2200 TU field emission microscope operating at an accelerating voltage of 200 kV. The diffuse reflectance spectra were measured using UV–vis spectrometer (Shimadzu, Japan, UV-2401 PC) using $BaSO_4$ as a reference.

Surface acidity of the system was determined using the pyridine adsorption method. Titania samples were first placed in a chamber saturated with pyridine atmosphere at 50 °C for a period of 48 h. The chamber was then evacuated using a vaccum pump for 2 h. These titania samples were then mixed with KBr with a concentration of 3% and pressed to pellets of diameter 10 mm. The analysis was carried out using an FTIR spectrophotometer (Nicolet Magna 500, Schimadzu, Japan). The Brϕnsted acidity was determined from TGA measurements using 2,6-dimethyl pyridine as a probe molecule as reported in the literature [48].

The photocatalytic activity of samples calcined at 800 °C was studied by measuring the amount of methylene blue degraded under UV irradiation. Aliquots were prepared by dispersing 0.1 g of titania powder in 250 ml of 6.4×10^{-9} mol l^{-1} methylene blue solution (AR grade, Qualigens Fine Chemicals, India). The suspension was equilibrated by stirring in the dark for 1 h prior to measurements to eliminate the error due to the adsorption of methylene blue on the titania surface. The initial concentration of methylene blue was measured only after equilibration. The suspension was then irradiated with UV light using a Rayonet photo reactor (Netherlands) with constant stirring. The UV source consisted of fifteen, 15 W tubes (Philips G15 T8) arranged in circular fashion emitting radiation in the region of 200–400 nm. The degradation of the dye was monitored after 60 min exposure using a UV–vis spectrometer (Shimadzu, Japan, UV-2401 PC). A blank dye solution was also irradiated for 1 h to confirm that the dye was not photo-bleached by the irradiation in the UV chamber. The absorption maximum between 640 and 680 nm in the spectrum of methylene blue was used to determine the concentration.

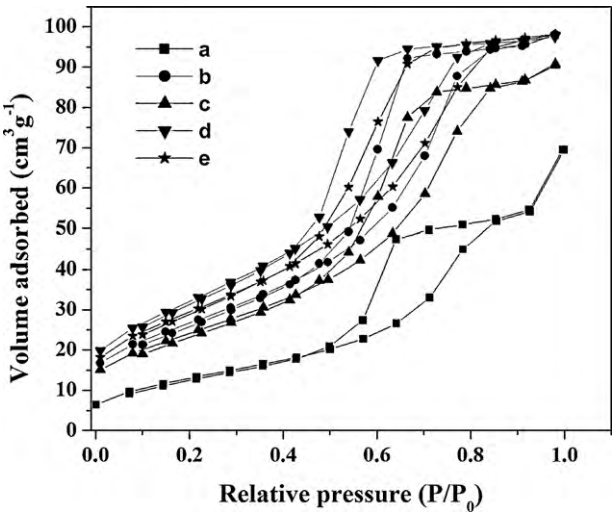

Fig. 1. Adsorption isotherm of: (a) pure titania (b) 1 mol% Gd_2O_3 doped TiO_2 (c) 2 mol% Gd_2O_3 doped TiO_2 (d) 5 mol% Gd_2O_3 doped TiO_2 (e) 10 mol% Gd_2O_3 doped TiO_2 calcined at 500 °C.

3. Results and discussion

Specific surface area (S_{BET}) and total pore volume data obtained from N_2 adsorption analyses and crystallite sizes obtained from XRD for the samples calcined at 500, 600, 700 and 800 °C are presented in Table 1. The adsorption isotherms (Fig. 1) of all the samples show type IV behaviour with the typical hysteresis loop. Undoped titania showed an upward tailing at higher relative pressure which is due to the wide distribution of mesopores with contribution from large pores beyond mesopore scale (>50 nm). The adsorption isotherm of gadolinium doped titania has a well defined narrow pore size distribution without any contribution of large pores beyond mesopore scale. The hysteresis loop obtained was an intermediate between H1 and H2 type, which confirms the gadolinium doped mesoporous titania has cylindrical mesopores having high degree of pore-size uniformity [49]. The pore size distribution curve also showed that the pores are in the mesoporous region (Fig. 2). It should be noted here, even for 1 mol% Gd doping, surface area value of titania is more than twice the value of undoped titania at all the temperatures (Table 1). With an increase in the calcination temperature the average pore size increased for all the samples due to the increase in crystallite size. Inter particle pores will be larger for larger particles. This is reflected in the surface area values and all the samples showed decrease in surface area with increasing calcination temperature (Fig. 3). The considerable decrease in pore volume appeared only when the calcination temperature reaches 800 °C (Table 1). This is because the rutile phase started to form at this temperature, which is clearly shown in Fig. 4 which is a plot of the rutile concentration against the calcination temperature. All the doped samples started to form the rutile phase around this temperature. In summary the doping of Gd yielded well defined mesopores at temperatures as high as 800 °C and increased the surface area compared to the undoped titania. The high surface

Table 1
Nitrogen adsorption characteristics of undoped and doped titania calcined at 500, 600, 700 and 800 °C.

Mol% doping	BET surface area ($m^2 g^{-1}$)	Total pore volume ($cm^3 g^{-1}$)	Micro pore volume ($cm^3 g^{-1}$)	Meso pore volume ($cm^3 g^{-1}$)	Crystallite size of anatase (nm)
Calcined 500 °C					
Undoped	48.7	0.1084	0.00392	0.1045	12.8
1 mol% Gd_2O_3 doped titania	97.7	0.1514	0.00221	0.1493	7.2
2 mol% Gd_2O_3 doped titania	88.5	0.1405	0.00265	0.1378	6.9
5 mol% Gd_2O_3 doped titania	117.9	0.1511	0.00414	0.147	6
10 mol% Gd_2O_3 doped titania	107.7	0.1517	0.003	0.1487	5.2
Calcined at 600 °C					
Undoped	19.1	0.0478	0.00015	0.0477	19.1
1 mol% Gd_2O_3 doped titania	71.5	0.1511	0.00039	0.1508	8.6
2 mol% Gd_2O_3 doped titania	57.6	0.1366	0.00096	0.1357	8.2
5 mol% Gd_2O_3 doped titania	81.8	0.1488	0.00114	0.1476	6.2
10 mol% Gd_2O_3 doped titania	88.9	0.1449	0.00285	0.1421	5.5
Calcined at 700 °C					
Undoped	8.6	0.0277	0.00007	0.0276	31.1
1 mol% Gd_2O_3 doped titania	35.1	0.0757	0.00112	0.0745	15.1
2 mol% Gd_2O_3 doped titania	32.8	0.0811	0.00122	0.07988	11.7
5 mol% Gd_2O_3 doped titania	40.2	0.0909	0.00015	0.09075	8.8
10 mol% Gd_2O_3 doped titania	51.5	0.1163	0.00123	0.11507	7.2
Calcined at 800 °C					
Undoped	0.3364	0.00096			37.5 (*R*)
1 mol% Gd_2O_3 doped titania	22.5	0.0351	0.00107	0.0341	19.2
2 mol% Gd_2O_3 doped titania	21.9	0.0428	0.00036	0.0424	16
5 mol% Gd_2O_3 doped titania	20.8	0.0353	0.00022	0.035	14.7
10 mol% Gd_2O_3 doped titania	15.3	0.0258	0.00041	0.0253	10.9

area was also retained even at 800 °C, at which temperature pure titania shows close to zero surface area.

The anatase to rutile ratio calculated using Spurr equation for all the samples calcined at different temperatures is presented in Fig. 4. All the gadolinium doped samples showed 100% anatase up to 700 °C, whereas in undoped titania only 29% anatase is observed. Undoped titania is transformed to 100% rutile at 800 °C (Fig. 5), whereas the doped samples only undergo complete phase transformation above 900 °C. The TiO_2 samples doped using 2 mol% Gd and above, remained completely in the anatase form even above 800 °C (Fig. 5). The crystallite size of the anatase phase against temperature for different titania samples is presented in Fig. 6. The crystallite size of the anatase phase is below 10 nm at 700 °C for samples containing gadolinium doping above 2 mol%. The reduction in the crystallite size is due to the segregation of the dopant cation at the grain boundary, which inhibits the grain growth by restricting the direct contact of anatase grains. The anatase phase is reported to be thermodynamically stable at very low particle sizes (below 14 nm). When the temperature increases, the crystallite size will increase and anatase phase will convert to the rutile phase. The rutile phase in both doped and undoped titania is formed when the crystallite size reaches a critical value of 12–20 nm, which is in accordance with the reported critical size [50,51]. It has also been reported that the rare earth ion in the titania matrix forms Ti–O–RE bonds which will inhibit the crystalline growth of titania [28]. Hence gadolinium effectively hinders the crystallite growth of anatase titania thereby stabilizing the anatase phase at temperatures above 800 °C. Another factor influencing the anatase to rutile transformation is oxygen vacancies produced during the calcination which act as nucleation centres for crystallite growth, which further promotes the phase transformation [14,52,53]. According to Shannon and Pask, a doping cation with an oxidation state of +3 or lower will go into the interstitial position of titania and decrease the oxygen vacancy concentration [14]. The gadolinium ion has a stable oxidation state of +3 and its ionic radius is 0.094 nm which is higher

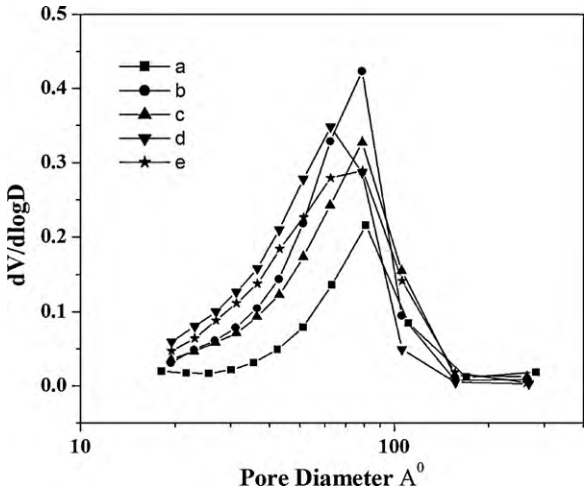

Fig. 2. Pore size distribution curve of: (a) pure titania (b) 1 mol% Gd_2O_3 doped TiO_2 (c) 2 mol% Gd_2O_3 doped TiO_2 (d) 5 mol% Gd_2O_3 doped TiO_2 (e) 10 mol% Gd_2O_3 doped TiO_2 calcined at 500 °C.

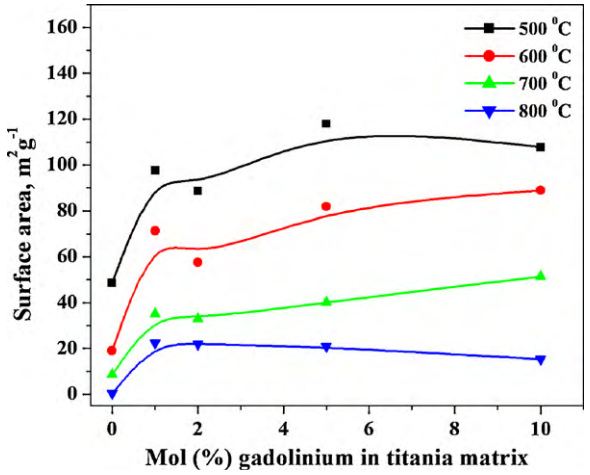

Fig. 3. Surface area of pure and gadolinium doped titania calcined at different temperature.

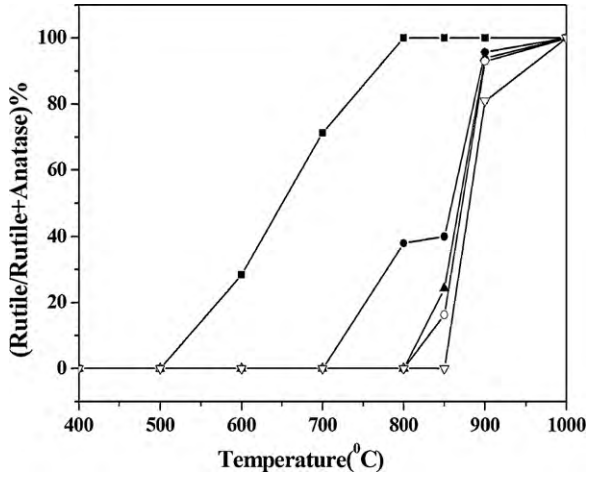

Fig. 4. Phase transformation from anatase to rutile of pure and Gd_2O_3 doped TiO_2 calcined at different temperatures for 1 h: (■) pure titania (●) 1 mol% Gd_2O_3 doped TiO_2 (▲) 2 mol% Gd_2O_3 doped TiO_2 (○) 5 mol% Gd_2O_3 doped TiO_2 (▽) 10 mol% Gd_2O_3 doped TiO_2.

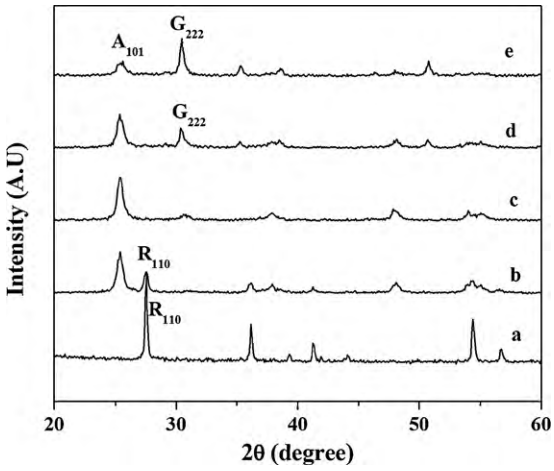

Fig. 5. XRD patterns of different TiO_2 samples calcined at 800 °C for 1 h: (A) anatase (R) rutile (G) $Gd_2Ti_2O_7$ (a) pure TiO_2 (b) 1 mol% Gd_2O_3 doped TiO_2 (c) 2 mol% Gd_2O_3 doped TiO_2 (d) 5 mol% Gd_2O_3 doped TiO_2 (e) 10 mol% Gd_2O_3 doped TiO_2. Anatase (1 0 1), rutile (1 1 0), $Gd_2Ti_2O_7$ (2 2 2) reflections are marked as A_{101}, R_{110}, G_{222} respectively.

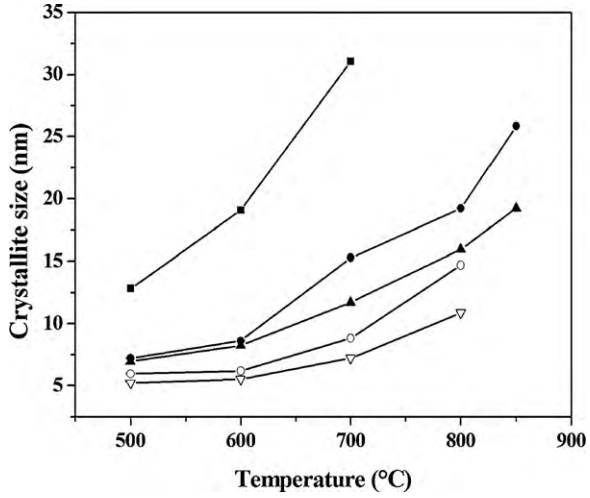

Fig. 6. Crystallite size of the anatase phase in pure and Gd_2O_3 doped TiO_2 calcined at different temperatures for 1 h: (■) pure titania (●) 1 mol% Gd_2O_3 doped TiO_2 (▲) 2 mol% Gd_2O_3 doped TiO_2 (○) 5 mol% Gd_2O_3 doped TiO_2 (▽) 10 mol% Gd_2O_3 doped TiO_2.

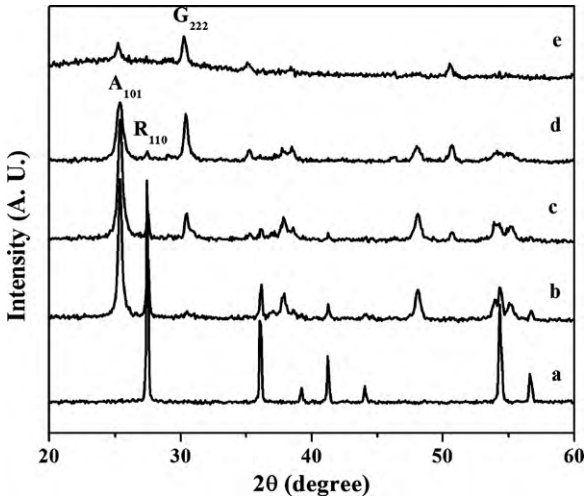

Fig. 7. XRD patterns of different TiO_2 samples calcined at 850 °C for 1 h: (A) anatase (R) rutile (G) $Gd_2Ti_2O_7$ (a) pure TiO_2 (b) 1 mol% Gd_2O_3 doped TiO_2 (c) 2 mol% Gd_2O_3 doped TiO_2 (d) 5 mol% Gd_2O_3 doped TiO_2 (e) 10 mol% Gd_2O_3 doped TiO_2. Anatase (1 0 1), rutile (1 1 0), $Gd_2Ti_2O_7$ (2 2 2) reflections are marked as A_{101}, R_{110}, G_{222} respectively.

than the ionic radius of Ti^{4+} (0.061 nm). Therefore in doped titania, the gadolinium ion is located in the interstitial position resulting in the hindering of the anatase to rutile phase transformation. This factor is well supported by the XRD studies. Moreover, the high ionic radius of the Gd^{3+} will induce a stress in the titania matrix and this is another reason for the high anatase to rutile phase transformation temperature. A similar observation was made by Ahmad et al. on Sc^{3+} doped titania [54]. With increasing concentration of Gd mol%, the formation of a new peak indexed to planes in the $Gd_2Ti_2O_7$ phase JCPDS card no 23-0259 (Figs. 5 and 7) begins to appear along with anatase phase. The main peak of $Gd_2Ti_2O_7$ corresponds to the (2 2 2) plane at a 2θ value 30.38°. On calcination at higher temperatures above 800 °C the anatase to rutile phase transformation occurs at an enhanced rate due to the presence of this additional phase $Gd_2Ti_2O_7$. Lin and Yu reported similar results for the anatase to rutile transformation in a mixture of titania and lanthanum oxide [31]. The XRD spectrum of the samples calcined at 800 and 850 °C (Figs. 5 and 7) showed the presence of $Gd_2Ti_2O_7$ phase. The intensity of the peaks corresponding to the $Gd_2Ti_2O_7$ is more pronounced in the X-ray diffraction pattern of the 5 and 10 mol% Gd doped samples (Figs. 5 and 7). This may be due to the high crystallinity of the $Gd_2Ti_2O_7$ compared to the anatase titania phase in the system. By comparing the intensity of 5 mol% Gd doped titania calcined at 850, 900 and 1000 °C (Supplementary information, Fig. 1), the $Gd_2Ti_2O_7$ peaks intensity decreases compared to the titania peak with increasing temperature. A similar type of high intensity peak ($Eu_2Ti_2O_7$ phase) is observed by Zhang et al. after heating Eu doped titania to 900 °C [55]. However, the intensity of $Gd_2Ti_2O_7$ in 10 mol% gadolinium doped titania calcined at 900 and 1000 °C found to be greater than the titania peaks (Supplementary information, Fig. 2). The UV–vis/diffuse reflectance spectroscopy was used to study the optical property of the pure and gadolinium doped titania calcined at 800 °C and the spectra are presented in Fig. 8. All the samples showed bands around 300–350 nm, due to presence of segregated anatase crystallites [56]. The undoped titania and 1 mol% Gd doped titania shows a 'red shift' due to the presence of rutile in the system which have a band gap of 3 eV. On increasing the concentration of gadolinium in the titania matrix, the 'band edge' shows a 'blue shift' due to the quantum size effects by reduction in size of the particles [57].

The TEM micrographs of undoped and 2 mol% gadolinium doped titania calcined at 800 °C were displayed in Fig. 9(A and B). The

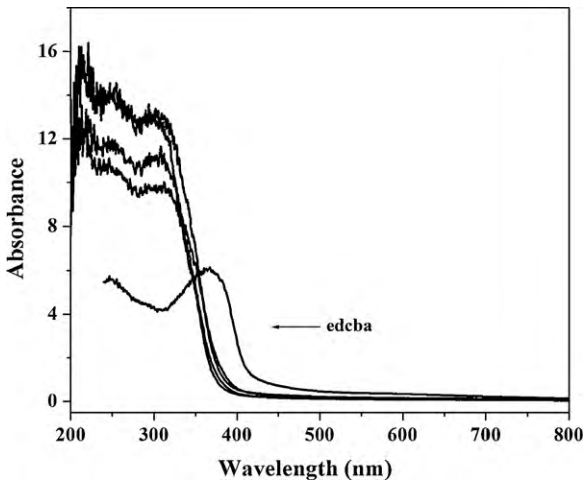

Fig. 8. DRS spectrum of TiO_2 samples calcined at 800 °C for 1 h: (a) pure TiO_2 (b) 1 mol% Gd_2O_3 doped TiO_2 (c) 2 mol% Gd_2O_3 doped TiO_2 (d) 5 mol% Gd_2O_3 doped TiO_2 (e) 10 mol% Gd_2O_3 doped TiO_2.

crystallite size measured from TEM images confirmed the lower crystallite size of gadolinium doped titania compared to pure titania. Undoped titania has a crystallite size of ~43 nm and 2 mol% gadolinium doped titania has a crystallite size of only ~20 nm. The HRTEM image shows well defined mesopores of anatase titania crystals with a small uniform size in doped titania, whereas the undoped titania shows agglomerated non-uniformly arranged large crystals (supplementary information, Fig. 3). From these observations it is clearly understood that the gadolinium in the titania matrix effectively hinders the crystalline growth of titania.

To understand the reactivity of the surface, the acidity of the doped and undoped titania system was examined using the pyridine adsorption technique [58]. Pyridine adsorbed on the doped and undoped titania (Fig. 10) showed bands at 1600–1630 cm^{-1} and 1460 cm^{-1} corresponding to the Lewis acid sites and a band at 1543 cm^{-1} corresponding to the formation of pyridinium ion on protonic sites, *i.e.* Brϕnsted acid sites [59]. These bands indicate the presence of Lewis and Brϕnsted acid sites in pure and gadolinium doped titania. Gadolinium doping increased the intensity of these peaks due to the large number of acidic sites created in the doped system in comparison with undoped titania. The reason for the higher number of acidic sites is due to the higher surface area and well defined mesopore structure present in the doped samples. Furthermore this Brϕnsted acidity of the samples was quantitatively investigated using the 2,6-dimethylpyridine adsorption method. This study is based on the previous literature report which showed that 2,6-dimethyl pyridine coordinates to the Brϕnsted acid sites of titania during adsorption and it desorbs from the acid sites when the temperature reaches above 300 °C [48,60]. Hence the Brϕnsted acidity was measured here by determining the weight loss of 2,6-dimethylpyridine in the temperature region 300–600 °C using thermo gravimetric analysis. The result obtained (Fig. 11) showed that gadolinium doping increased the Brϕnsted acidity of titania. The maximum Brϕnsted acidity was exhibited by 2 mol%

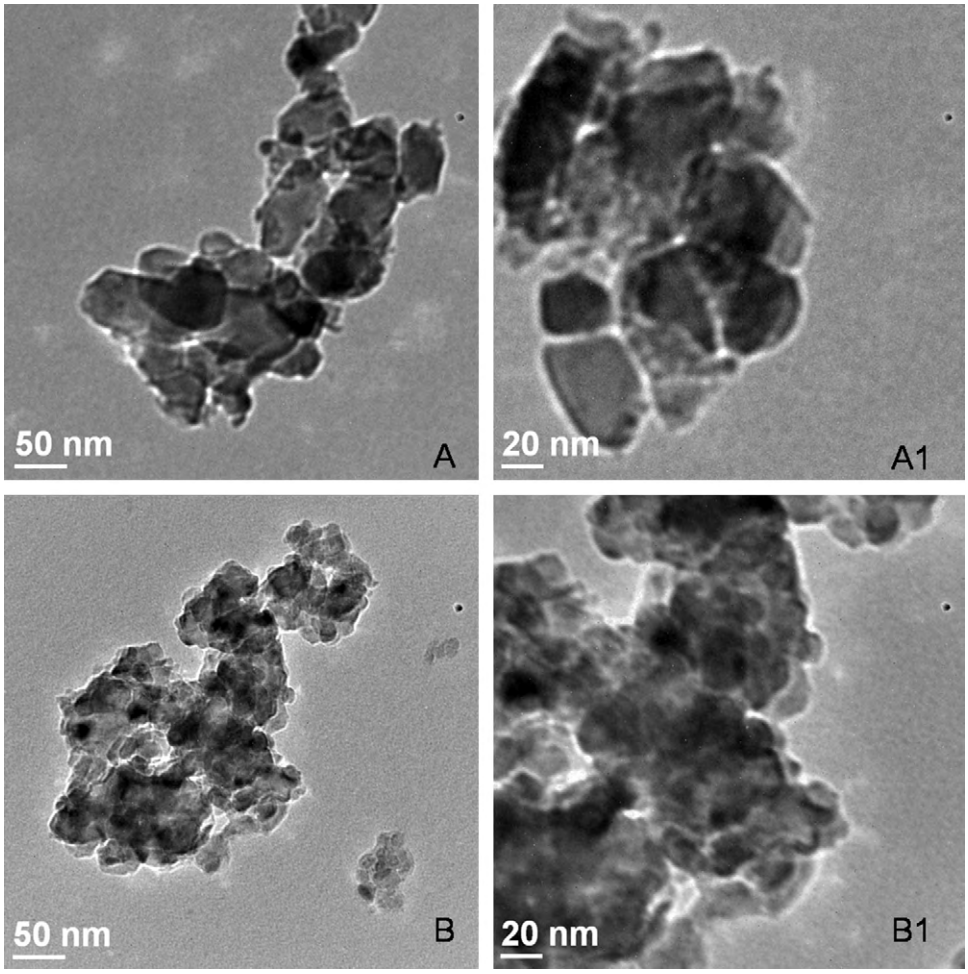

Fig. 9. TEM and HRTEM images of pure and doped titania calcined at 800 °C (A and A_1) undoped titania (B and B_1) 2 mol% gadolinium doped titania.

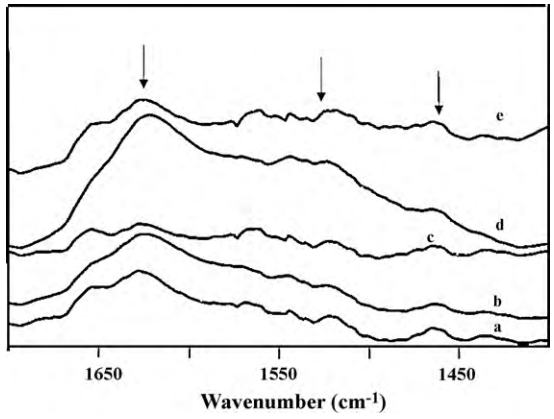

Fig. 10. Pyridine adsorption studies on: (a) pure titania (b) 1 mol% Gd_2O_3 doped TiO_2 (c) 2 mol% Gd_2O_3 doped TiO_2 (d) 5 mol% Gd_2O_3 doped TiO_2 (e) 10 mol% Gd_2O_3 doped TiO_2 calcined at 600 °C.

gadolinium doped titania, above 2 mol% the result was more or less similar.

The photocatalytic activity of pure and doped titania calcined at 800 °C measured using the methylene blue degradation studies are presented in Fig. 12. All the Gd doped samples showed significantly higher photocatalytic activity than the undoped titania. The gadolinium doped samples calcined at 800 °C, the 5 mol% doped samples showed the highest activity. Above 5 mol% doping there is a decrease in the photocatalytic activity observed. The photocatalytic activity decreased for gadolinium doped titania at 800 °C in the order of 5 mol% > 2 mol% > 1 mol% > 10 mol% > pure titania. The increased photocatalytic activity of gadolinium doped samples is due to higher surface area and anatase phase stability of the gadolinium doped sample. Interfacial charge transfer to the 4f level effectively reduced the electron–hole recombination for gadolinium doped samples. Gadolinium ions could act as an effective electron scavenger to trap the conduction band electrons of titania during the photocatalytic reaction [61]. Gadolinium doped samples have higher surface area than the undoped titania at all the temperatures. Moreover, with the exception of undoped and 1 mol%, gadolinium doped titania exists completely in the anatase phase at 800 °C. The decrease in surface area and formation of a secondary impurity phase ($Gd_2Ti_2O_7$) plays a major role in decreasing the photocatalytic activity of 10 mol% Gd doped sample. However, all the gadolinium doped titania samples

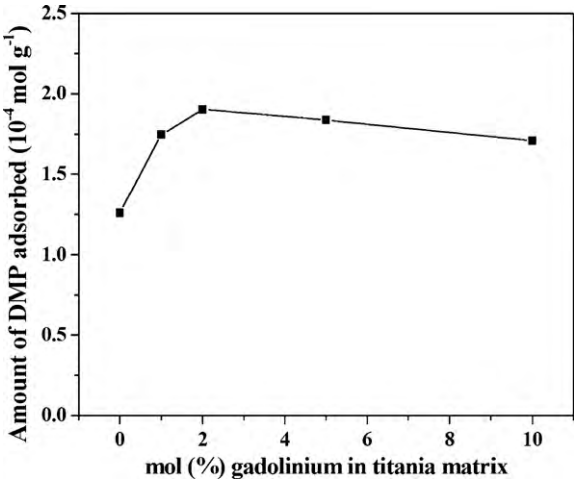

Fig. 11. Amount of DMP adsorbed versus gadolinium concentration in titania matrix.

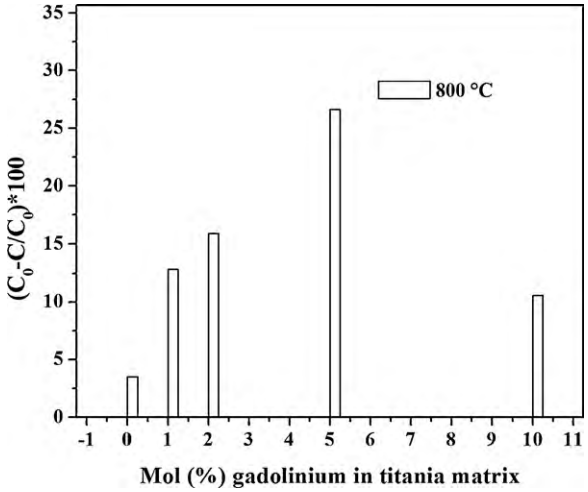

Fig. 12. Photocatalytic degradation profile of gadolinium doped and undoped titania.

show significantly higher photocatalytic activity than the undoped titania.

4. Conclusions

Mesoporous gadolinium doped nanocrystalline titania was prepared using an aqueous sol–gel method. The adsorption isotherm and HRTEM study confirmed that the gadolinium doped mesoporous titania has cylindrical mesopores having a high degree of pore-size uniformity. The BET surface area measurements showed that the surface area of the gadolinium doped titania is significantly higher than undoped titania at all the temperatures. For example, the surface area value of undoped titania is almost zero after calcination at 800 °C whereas the 1 mol% gadolinium doped titania has a surface area value of 22.5 $m^2\ g^{-1}$. The anatase to rutile phase transformation occurs in gadolinium doped and undoped titania when the crystallite size of anatase phase reaches the critical size of between 12 and 20 nm. Moreover, the anatase phase stability of the Gd doped titania was increased up to 900 °C. The photocatalytic activity of all the gadolinium doped samples showed significantly higher photocatalytic activity than undoped titania.

Acknowledgments

The authors acknowledge the members of Materials and Minerals division for providing general assistance. The authors Baiju K.V., Shajesh P. and Jaimy K.B. are grateful to CSIR, India, for providing financial support. Special thanks to Dr. Eoin Murray of School of Chemical Sciences, Dublin City University, for correcting the English in the manuscript.

Appendix A. Supplementary data

Supplementary data associated with this article can be found, in the online version, at doi:10.1016/j.jallcom.2010.06.028.

References

[1] M.S. Wainwright, N.R. Foster, Catal. Rev. 19 (1979) 211.
[2] Y. Paz, Z. Luo, L. Rabenberg, A. Heller, J. Mater. Res. 10 (1995) 2842.
[3] A. Fujishima, T.N. Rao, D.A. Tryk, J. Photochem. Photobiol. C 1 (2000) 1.
[4] P. Periyat, D.E. Mccormack, S.J. Hinder, S.C. Pillai, J. Phys. Chem. C 113 (2009) 3246.
[5] J. Wang, Z. Wang, H. Li, Y. Cui, Y. Du, J. Alloys Compd. 494 (2010) 372.
[6] J. Wang, W. Zhu, Y. Zhang, S. Liu, J. Phys. Chem. C 111 (2007) 1010.
[7] H. Xia, H. Zhuang, D. Xiao, T. Zhang, J. Alloys Compd. 465 (2008) 328.

[8] Y. Lv, L. Yua, H. Huang, H. Liu, Y. Feng, J. Alloys Compd. 488 (2009) 314.
[9] M.-S. Wong, S.-W. Hsu, K.K. Rao, C.P. Kumar, J. Mol. Catal. A: Chem. 279 (2008) 20.
[10] Y. Yang, J.M.F. Ferreira, Mater. Lett. 36 (1998) 320.
[11] P. Periyat, K.V. Baiju, P. Mukundan, P.K. Pillai, K.G.K. Warrier, Appl. Catal. A 349 (2008) 13.
[12] V. Guidi, M.C. Carotta, M. Ferroni, G. Martinelli, M. Sacerdoti, J. Phys. Chem. B 107 (2003) 120.
[13] P. Periyat, K.V. Baiju, P. Mukundan, P.K. Pillai, K.G.K. Warrier, J. Sol–Gel Sci. Technol. 43 (2007) 299.
[14] R.D. Shannon, J.A. Pask, J. Am. Ceram. Soc. 48 (1965) 391.
[15] S. Karvinen, R.J. Lamminmaki, Solid State Sci. 5 (2003) 1159.
[16] M. Anpo, M. Takeuchi, J. Catal. 216 (2003) 505.
[17] K.Y. Jung, S.B. Pask, Appl. Catal. B 25 (2000) 249.
[18] A. Rampaul, I.P. Parkin, S.A. O'Neill, J. Desouza, A. Mills, N. Elliott, Polyhedron 22 (2003) 35.
[19] J. Moon, H. Takagi, Y. Fujishiro, M. Awano, J. Mater. Sci. 36 (2001) 949.
[20] S. Janitabar-Darzi, Ali Reza Mahjoub, J. Alloys Compd. 486 (2009) 805.
[21] M. Toyoda, Y. Nanbu, Y. Nakazawa, M. Hirano, M. Inagaki, Appl. Catal. A 49 (2004) 227.
[22] K.T. Ranjit, I. Willner, S.H. Bossmann, A.M. Braun, Environ. Sci. Technol. 35 (2001) 1544.
[23] J. Nair, P. Nair, F. Mizukami, Y. Oosawa, T. Okubo, Mater. Res. Bull. 34 (1999) 1275.
[24] R.M. Mohamed, I.A. Mkhalid, J. Alloys Compd. (2010), doi:10.1016/j.jallcom.2010.04.061.
[25] C.A. LeDuc, J.M. Campbell, J.A. Rosssin, Ind. Eng. Chem. Res. 35 (1996) 2473.
[26] R. Gopalan, Y.S. Lin, Ind. Eng. Chem. Res. 34 (1995) 1189.
[27] E. Setiawati, K. Kawano, J. Alloys Compd. 451 (2008) 293.
[28] C.P. Sibu, S. Rajesh Kumar, P. Mukundan, K.G.K. Warrier, Chem. Mater. 14 (2002) 2876.
[29] T. Peng, D. Zhao, H. Sing, C. Yan, J. Mol. Catal. A: Chem. 238 (2005) 119.
[30] Y. Xie, C. Yuan, Appl. Surf. Sci. 221 (2004) 17.
[31] J. Lin, J.C. Yu, J. Photochem. Photobiol. A 116 (1998) 63.
[32] T.D. Nguyen-Phan, M.B. Song, E.W. Shin, J. Hazard. Mater. 167 (2009) 75.
[33] L. Li, C.-K. Tsung, Z. Yang, G.D. Stucky, L. Sun, J. Wang, C. Yan, Adv. Mater. 20 (2008) 903.
[34] K.L. Frindell, M.H. Bartl, M.R. Robinson, G.C. Bazan, A. Popitsch, G.D. Stucky, J. Solid State Chem. 172 (2003) 81.
[35] W. Zhou, Y. Zheng, G. Wu, Appl. Surf. Sci. 253 (2006) 1387.
[36] J. Zhao, C. Jia, H. Duan, Z. Sun, X. Wang, E. Xie, J. Alloys Compd. 455 (2008) 497.
[37] B. Yang, Z. Zhu, Y. Zhou, C. Xia, J. Sci. Conf. Proc. 1 (2009) 243.
[38] J. Zhu, J. Xie, M. Chen, D. Jiang, D. Wu, Colloids Surf. A 355 (2010) 178.
[39] S. Hishita, I. Mutoh, K. Koumoto, H. Yanagida, Ceram. Int. 9 (1983) 61.
[40] D. Zhao, T. Peng, M. Liu, L. Lu, P. Cai, Micropor. Mesopor. Mater. 114 (2008) 166.
[41] Y. Zhang, H. Zhang, Y. Xu, Y. Wang, J. Solid State Chem. 177 (2004) 3490.
[42] Z.M. El-Bahy, A.A. Ismail, R.M. Mohamed, J. Hazard. Mater. 166 (2009) 138.
[43] V. Stengl, S. Bakardjieva, N. Murafa, Mater. Chem. Phys. 114 (2009) 217.
[44] M. Zalas, B. Gierczyk, M. Laniecki, Pol. J. Chem. 82 (2008) 1767.
[45] H.S. Hafez, M. Saif, J.T. McLeskey Jr., M.S.A. Abdel-Mottaleb, I.S. Yahia, T. Story, W. Knoff, Int. J. Photoener. (2009) 1–8.
[46] R.A. Spurr, H. Myers, Anal. Chem. 29 (1957) 760.
[47] S. Ghosh, D. Divya, K.C. Remani, T.S. Sreeremya, J. Nanopart. Res. 12 (2010) 1905.
[48] K.R. Sunajadevi, S. Sugunan, Mater. Lett. 58 (2004) 3290.
[49] S.J. Gregg, K.S.W. Sing, Adsorption, Surface Area and Porosity, IInd ed., Academic Press, 1982.
[50] H. Zhang, J.F. Banfield, J. Mater. Chem. 8 (1998) 2073.
[51] A.A. Gribb, J.F. Banfield, Am. Min. 82 (1997) 717.
[52] F.C. Gennari, D.M. Pasquevich, J. Mater. Sci. 33 (1998) 1571.
[53] K.N.P. Kumar, K. Keizer, A.J. Burggraaf, J. Mater. Chem. 3 (1993) 1141.
[54] A. Ahmad, J.A. Shah, S. Buzby, S.I. Shah, Eur. J. Inorg. Chem. (2008) 948.
[55] Y. Zhang, H. Zhang, Y. Xu, Y. Wang, J. Mater. Chem. 13 (2003) 2261.
[56] A.M. Prakash, H.M. Sung-Suh, L. Kevan, J. Phys. Chem. B 102 (1998) 857.
[57] L.E. Brus, J. Chem. Phys. 79 (1983) 5566.
[58] J. Ryezkowski, Catal. Today 68 (2001) 263.
[59] G. Bosca, Catal. Today 41 (1998) 191.
[60] A. Satsuma, Y. Kamiya, Y. Westi, T. Hattori, Appl. Catal. A 194 (2000) 253.
[61] H. Liu, X.Z. Li, Y.J. Leng, W.Z. Li, J. Phys. Chem. B 107 (2003) 8988.